PHYSICAL REVIEW B **76**, 020509(R) (2007)

Quantum phase diagram of antiferromagnetism and superconductivity with a tetracritical point in $CeRhIn_5$ in zero magnetic field

M. Yashima,[1] S. Kawasaki,[1] H. Mukuda,[1] Y. Kitaoka,[1] H. Shishido,[2] R. Settai,[2] and Y. Ōnuki[2,3]
[1]*Department of Materials Engineering Science, Osaka University, Osaka 560-8531, Japan*
[2]*Department of Physics, Graduate School of Science, Osaka University, Osaka 560-0043, Japan*
[3]*Advanced Science Research Center, Japan Atomic Energy Research Institute, Tokai, Ibaraki 319-1195, Japan*
(Received 6 June 2007; published 20 July 2007)

We report on a pressure-temperature phase diagram of antiferromagnetism (AFM) and superconductivity (SC) in $CeRhIn_5$ studied by the nuclear-quadrupole-resonance measurements under pressure. It is demonstrated that an AFM phase transition takes place inside the superconducting state. This result reveals that a tetracritical point exists in the phase diagram of AFM and SC at zero magnetic field. The finding of unconventional SC characteristics in the uniformly coexisting phase of AFM and SC suggests that both phases may be mediated by the same magnetic interaction.

DOI: 10.1103/PhysRevB.76.020509 PACS number(s): 74.25.Ha, 74.62.Fj, 74.70.Tx, 75.30.Kz

A number of studies on strongly correlated *f* electron systems revealed that unconventional superconductivity (SC) arises at or close to a quantum critical point (QCP), where magnetic order disappears at low temperature (T) as a function of lattice density via application of hydrostatic pressure (P).[1] These findings suggest that the mechanism forming Cooper pairs can be magnetic in origin. Namely, on the verge of magnetic order, the magnetically soft electron liquid can mediate spin-dependent attractive interactions between the charge carriers.[2] The phase diagram, schematically shown in Fig. 1(a), has been observed in antiferromagnetic heavy-fermion (HF) compounds such as $CeIn_3$,[2] $CePd_2Si_2$,[3] and $CeRh_2Si_2$.[4,5] In $CeIn_3$ (Ref. 6) and $CeRh_2Si_2$,[5] the P-induced first-order transition from antiferromagnetism (AFM) to paramagnetism (PM) has been revealed near the boundary where SC emerges without the development of antiferromagnetic spin fluctuations. Remarkably different behavior, schematically shown in Fig. 1(b), has been found in the archetypal HF superconductor $CeCu_2Si_2$ (Refs. 7 and 8) and the more recently discovered $CeRhIn_5$.[9,10] Although an analogous behavior relevant with an AFM-QCP has been demonstrated in both the compounds, it is noteworthy that the associated superconducting region extends to higher densities than in the other compounds, their value of T_c reaching its maximum away from the verge of AFM.[10–12]

Recently, nuclear-quadrupole-resonance (NQR) and ac-susceptibility measurements indicated that AFM coexists uniformly with SC on a microscopic level in the range $P=1.60-1.75$ GPa in $CeRhIn_5$.[13,14] An issue is which type of quantum-phase transition (QPT), either a first or a second order, thermodynamically takes place from the AFM+SC uniformly coexisting phase to the paramagnetic SC phase in $CeRhIn_5$ as a function of P. The specific-heat measurements are indicative of a first-order transition around $P_c \sim 2.0$ GPa from the sudden disappearance of anomaly relevant with the AFM above P_c.[15,16] This indicates that when $T_c > T_N$, AFM is hidden and hence both phases compete with one another. It was reported that a line of QPT's is induced inside the superconducting state by an applied magnetic field.[15,16] An inevitable experimental difficulty is that we cannot apply a completely homogeneous pressure to the sample, preventing any previous experiments from identifying a line separating the AFM+SC uniformly coexisting phase from the paramagnetic SC phase when T_N sharply collapses into zero.

The single crystals of $CeRhIn_5$ grown by the self-flux method were moderately crushed into a large size of grains in order to make RF pulses for NQR measurements penetrate into the samples easily. Hydrostatic pressure was applied by utilizing a NiCrAl-BeCu piston-cylinder cell, filled with Si-based organic liquid as a pressure-transmitting medium. To calibrate the pressure at low temperatures, the shift in T_c of Sn metal under P was monitored by the resistivity measurement. The ^{115}In($I=9/2$)-NQR spectrum measurements are performed at the transition of $1\nu_Q$ ($\pm 1/2 \leftrightarrow \pm 3/2$) for the ^{115}In(1) site in $CeRhIn_5$. $CeRhIn_5$ consists of alternating layers of $CeIn_3$ and $RhIn_2$ and hence has two different In sites per one unit cell. The In(1) site, analogous to the In site in $CeIn_3$, is located on the top and bottom faces of the tetragonal unit cell. Here ν_Q is defined by the NQR Hamiltonian, $\mathcal{H}_Q=(h\nu_Q/6)[3I_z^2-I(I+1)+\eta(I_x^2-I_y^2)]$, where η is an asymmetry parameter of the electric field gradient [$\nu_Q=6.87$ MHz and $\eta=0$ at In(1) and $P=0$]. When AFM occurs, the Hamiltonian of ^{115}In nuclei is replaced by $\mathcal{H}_{\mathrm{AFM}}=-\gamma h\vec{I}\cdot\vec{B}+\mathcal{H}_Q$, where $\vec{B}$ is the internal magnetic field. We can identify the onset of AFM from the splitting of the

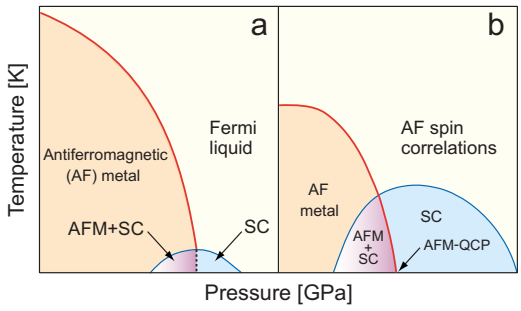

FIG. 1. (Color online) Schematic phase diagrams of HF compounds. (a) The P-T phase diagram for $CePd_2Si_2$, $CeIn_3$, and $CeRh_2Si_2$. (b) The P-T phase diagram for $CeCu_2Si_2$ and $CeRhIn_5$.

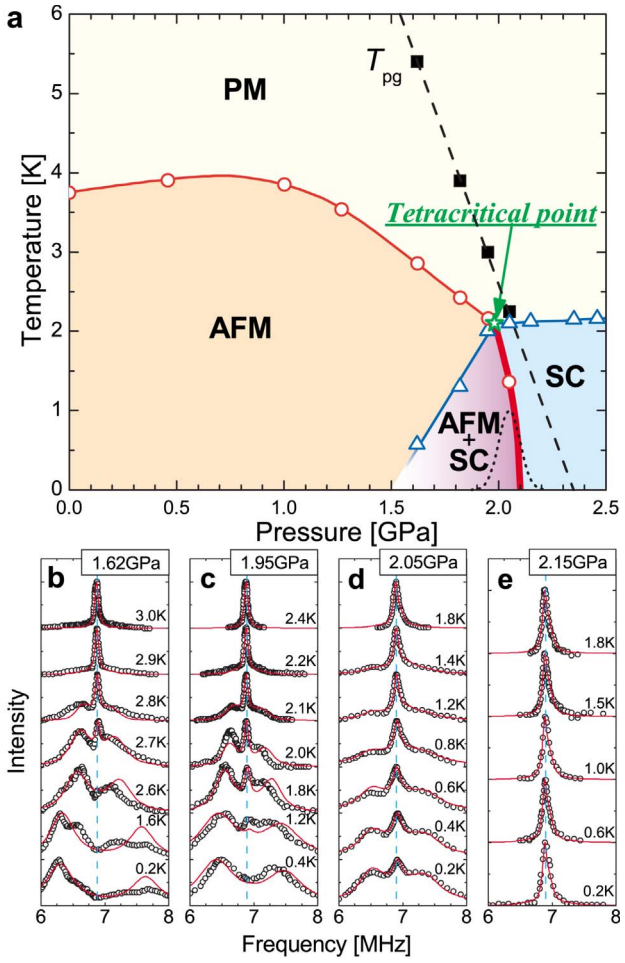

FIG. 2. (Color online). (a) The pressure-temperature phase diagram constructed from the NQR measurements. The thin and thick red curves are the respective T_N lines of the pure AFM phase and the AFM+SC uniformly coexisting phase. We obtained the P dependence of T_N from the present experiment as $T_N(P)=-\frac{25}{12}(P-1.98)+2.1$ for $1.4\ \text{GPa}<P<1.98\ \text{GPa}$ and $T_N(P)=2.1\left(\frac{2.1-P}{2.1-1.98}\right)^{1/2}$ for $1.98\ \text{GPa}<P$. The blue line is a guide for the eyes for the P dependence of T_c. All T_c data are obtained from the T_1 measurements. The star denotes the position of the tetracritical point. The AFM+SC uniformly coexisting phase is denoted in the pressure-temperature region colored by purple. The pseudogap temperature (T_{pg}) is shown by a square (Ref 14). The dotted curve shows GDP with $\Delta P=0.07$ GPa at $P_0=2.05$ GPa. (b), (c), (d), and (e) indicate the temperature dependence of ^{115}In-NQR spectrum of $1_{\nu Q}$ for different pressures. The dotted line indicates a peak position at which the NQR spectrum is observed for PM. The solid red lines are the spectra calculated by incorporating the distribution of pressure $\Delta P=0.07$ GPa.

$1\nu_Q$ spectrum in association with the appearance of internal field.

Figure 2(b) presents the T dependence of NQR spectra at $P=1.62$ GPa. Below $T\sim 3$ K, the NQR spectra reveal a mixture of both domains of AFM and PM in a narrow range of $T=2.7-2.9$ K. This mixture is associated with a distribution of T_N originating from an inevitable distribution in P, revealing that the application of P is not always homogeneous in

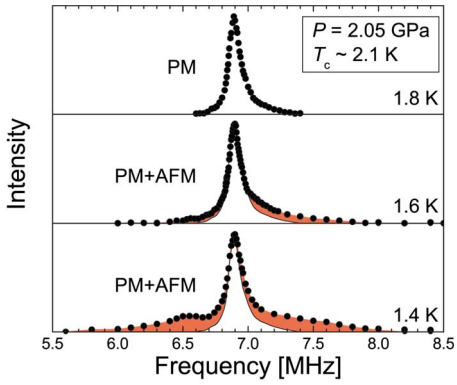

FIG. 3. (Color online) Temperature dependence of ^{115}In-NQR spectrum of $1_{\nu Q}$ below $T_c=2.1$ K at $P=2.05$ GPa. The solid lines indicate the spectrum at 1.8 K.

fact. When keeping this experimental situation in mind, we analyze the NQR spectra at $P=1.62$ GPa to estimate an "*in situ*" distribution of P. The T variation of NQR spectra in Fig. 2(b) is well reproduced, noting several issues described below. The T dependence of the internal field (H_{int}), that is induced by AFM moments, is described in terms of a molecular field model for spin=1/2, given by $S_Q=\tanh(S_Q/t)$ where $S_Q=M_Q(T)/M_Q(0)$ and $t=T/T_N$. Here $M_Q(T)$ is an AFM ordered moment at T. $M_Q(P)$ decreases according to the relation of $M_Q\propto T_N^{3/4}$ around the AFM-QCP in HF systems.[17] A Gaussian distribution of pressure (GDP) inside the sample is assumed by the relation of $\text{GDP}(P)\propto\exp\left[-\left(\frac{P-P_0}{\Delta P}\right)^2\right]$, where ΔP and P_0 indicate a pressure distribution inside the sample and a mean value of P in the pressure cell, respectively. For fitting the T variation of the spectra in Fig. 2(b), we used the parameters of $T_N=2.85$ K, $H_{\text{int}}(T=0)\sim 290$ Oe and a slope of $\partial T_N/\partial P\sim -2.1$ K/GPa [see Fig. 2(a)]. As a result, the calculated spectra are displayed by red lines in Fig. 2(b), allowing to estimate quantitatively $\Delta P=0.07$ GPa.

Figures 2(c)–2(e) show the T dependence of NQR spectra at $P=1.95$, 2.05, and 2.15 GPa, respectively. The mixed spectra of AFM and PM domains due to $\Delta P=0.07$ GPa is evident from 2.2 K to 1.2 K at $P=1.95$ GPa, indicating that T_N rapidly decreases beyond $P=1.95$ GPa. Remarkably, the mixed spectra of AFM and PM domains due to $\Delta P=0.07$ GPa [see the dotted curve in Fig. 2(a)] survives even down to 0.2 K below $T_N=1.3$ K at $P=2.05$ GPa, demonstrating that T_N vanishes just above $P=2.05$ GPa. Note that the AFM completely disappears at $P=2.15$ GPa because the NQR spectra do not reveal any splitting down to 0.2 K in association with the onset of AFM as shown in Fig. 2(e). In order to demonstrate the existence of the AFM boundary inside the SC dome, Fig. 3 shows the T dependence of the NQR spectrum below $T_c=2.1$ K at $P=2.05$ GPa. $CeRhIn_5$ stays in the PM-SC state at $T=1.8$ K because a single sharp NQR spectrum is observed. Upon cooling below $T=1.6$ K, however, the NQR spectrum starts to broaden due to the onset of AFM. In the P range in concern, since T_c is almost kept at $T_c=2.1$ K, we highlight that the AFM takes place in the SC phase well below $T_c\sim 2.1$ K as shown in Fig. 2(a). To

make one further convinced of the presence of the AFM+SC phase for $T_c > T_N$, the respective NQR spectra at $P=1.95$, 2.05, and 2.15 GPa are in excellent agreement with the spectra (red lines) calculated by assuming P variations of T_N depicted by the red line in Fig. 2(a). Most importantly, we have revealed from the microscopic NQR probe that the AFM is not hidden in the superconducting state at zero field even when $T_c > T_N$ and the AFM-QCP exists in the SC regime at $P_{QCP} \sim 2.1$ GPa. Namely, the present experiment gives microscopic evidence for the existence of a tetracritical point where the pure AFM, the AFM+SC uniformly coexisting phase, the paramagnetic SC, and the PM contact with each other at $T_{tetra} \sim 2.1$ K and $P_{tetra} \sim 1.98$ GPa. The P-induced QPT has thus been demonstrated to be of second order. As a matter of fact, either T_c or T_N decreases dramatically, but continuously with the pressure in the AFM+SC uniformly coexisting phase. This fact suggests that both order parameters are intimately connected with one another as if they were derived from the same magnetic interaction among electrons. We note that the SO(5) theory unifies AFM and SC states by a symmetry principle and describes their rich phenomenology through a single low-energy effective model,[18,19] and hence may deserve to describe the zero-field QPT of AFM and SC involving the tetracritical point.

Next, we deal with the unusual SC behavior in the AFM+SC uniformly coexisting phase. At $P=2.05$ GPa, $1/T_1$ follows a T^3 law ($1/T_1T \propto T^2$) down to 0.4 K, consistent with a line-node SC gap model as seen in Fig. 4(a). By contrast, at low temperatures, it deviates from the T^3-like behavior and exhibits a T-linear one even at $P=2.35$ GPa where a single SC state is established.[20,21] We note that a magnitude of $1/T_1T$ successively increases as P decreases in the AFM+SC uniformly coexisting phase [see the inset of Fig. 4(a)]. It is unexpected that the $1/T_1$ below $T_c=0.55$ K does not follow a T^3 dependence, but it is dominated by the T_1T-constant behavior at $P=1.62$ GPa. At first, we wonder if such a T_1T-constant behavior may be due to some impurity effect. In fact, recent theoretical work[22] argued that, in the AFM+SC uniformly coexisting phase, residual density of states could be enhanced due to the impurity scattering through introducing additional nodes in the superconducting gap function caused by the crossing of the Fermi surface with a magnetic Brillouin zone. This model is, however, not consistent with the experimental fact that $1/T_1$ obeys an apparent T^3 behavior below T_c in UPd_2Al_3 (Ref. 23) which homogeneously coexists with AFM. Therefore, it is unlikely that the enhancement of $1/T_1T$-constant contribution is associated with some impurity effect. Also, we rule out a possibility that a mismatch between an incommensurate antiferromagnetic order and SC brings about the gapless feature. This is because the incommensurate antiferromagnetic order evolves into a commensurate one before entering the AFM+SC uniformly coexisting phase revealed from an intimate change in NQR spectra.[24]

As a result, this increase in $1/T_1T$-constant contribution is concluded to be intrinsic in origin for the AFM+SC phase in $CeRhIn_5$. Here, note that the T_1T-constant behavior observed in the PM-SC phase at $P=2.35$ GPa is shown to be due to the inevitable impurity effect as well as in the case for $CeCoIn_5$.[25] In $CeRhIn_5$, one $4f$ electron per Ce atom contributes to both phases, forming the quantum states through the hybridization with conduction electrons. The particular situation that one $4f$ electron per Ce atom plays an essential role for the AFM+SC uniformly coexisting phase may cause the gapless nature in the low-lying excitations spectrum of quasiparticles through a close connection between both order parameters. By contrast, in UPd_2Al_3 with multiple $5f$ electrons per U, two of the $5f$ electrons contribute to both phases and a T^3 law in $1/T_1$ is valid even in the AFM+SC uniformly coexisting phase. In this context, the AFM+SC uniformly coexisting phase may differ in origin between Ce- and U-based compounds. Actually, similar P dependence of the T_1T-constant contribution was also observed in Ge-substituted $CeCu_2Si_2$.[8]

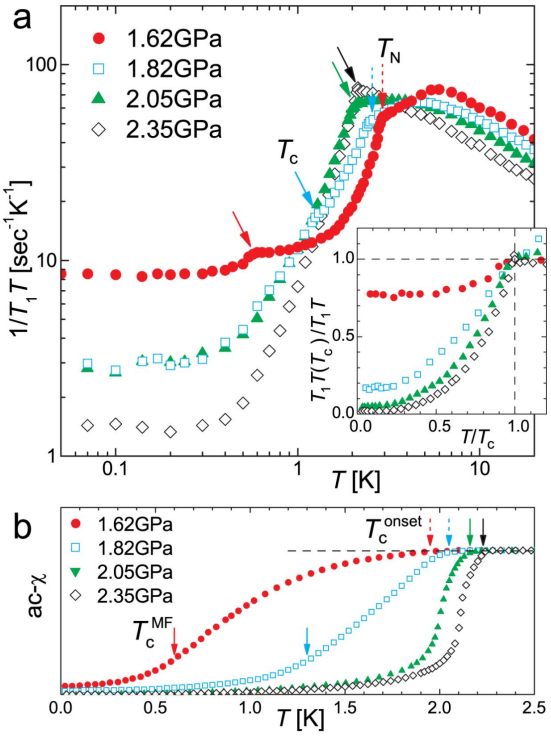

FIG. 4. (Color online). (a) The temperature dependence of $1/T_1T$ for various pressures in $CeRhIn_5$. The solid and dashed arrows indicate T_c and T_N, respectively. The simultaneous observations of T_c and T_N evidences the AFM+SC uniformly coexisting phase. Note that a clear reduction in $1/T_1T$ associated with the onset of AFM order is not observed below $T_N=1.3$ K at $P=2.05$ GPa. This is because the rapid decrease of T_N near the tetracritical point makes the antiferromagnetic transition broad. The inset presents plots of $T_1T(T_c)/T_1T$ vs T/T_c, indicating that a magnitude of $1/T_1T$ at low T depends on P for the AFM+SC uniformly coexisting phase. (b) The temperature dependence of the ac susceptibility measured with the same *in situ* NQR coil for different pressures in $CeRhIn_5$. The ac susceptibility is normalized by its value at 2.4 K for each pressure. The solid and dashed arrows indicate T_c^{MF} and T_c^{onset}, respectively. T_c^{MF} is estimated from the T_1 measurement. The dashed line is a guide for the eyes.

It is remarkable that the superconducting transition width in the ac-susceptibility becomes broader as P decreases from P_{tetra} (~ 1.98 GPa) to 1.62 GPa as shown in Fig. 4(b). Unex-

pectedly, $T_c^{\text{onset}} \sim 2$ K at $P=1.62$ and 1.82 GPa, defined as the temperature below which the diamagnetism starts to appear, is much higher than T_c^{MF}. However, any signature for the onset of SC from the $1/T_1$ measurements is not evident in between T_c^{onset} and T_c^{MF}, demonstrating that the mean-field type of gap does not open in this T range. In this context, the intimate interplay between AFM and unconventional SC on a single $4f$ electron per Ce may induce the fluctuations of the amplitude of superconducting order parameter below T_c^{onset}, leading to a broad transition toward SC that coexists with AFM. Furthermore, we have confirmed the pseudogap behavior as shown in Fig. 2(a). Many interesting phenomena including the gapless nature, the broad superconducting transition width in the ac susceptibility, and the pseudogap behavior have been observed around the tetracritical point, indicating that they are closely related to each other through the intimate interplay between AFM and unconventional SC.

In conclusion, the discovery of the tetracritical point at zero field presented here has shed light on the intimate relationship between AFM and SC, namely, both phases may be mediated by the same magnetic interaction. The P-induced systematic evolution of the gapless nature in the AFM+SC uniformly coexisting phase may be because both the order parameters of AFM and SC are not independent but intimately connected with one another. Superconductivity, which was one of the best understood many-body problems in physics, became again a challenging problem.

This work was supported by a Grant-in-Aid for Creative Scientific Research (Grant No. 15GS0213) from the Ministry of Education, Culture, Sports, Science, and Technology (MEXT) and the 21st Century COE Program (G18) by Japan Society of the Promotion of Science (JSPS).

[1] Y. Kitaoka *et al.*, J. Phys. Soc. Jpn. **74**, 186 (2005), and references therein.
[2] N. D. Mathur *et al.*, Nature (London) **394**, 39 (1998).
[3] F. M. Grosche *et al.*, Physica B **223&224**, 50 (1996).
[4] R. Movshovich, T. Graf, D. Mandrus, J. D. Thompson, J. L. Smith, and Z. Fisk, Phys. Rev. B **53**, 8241 (1996).
[5] S. Araki *et al.*, J. Phys.: Condens. Matter **14**, L377 (2002).
[6] S. Kawasaki *et al.*, J. Phys. Soc. Jpn. **73**, 1647 (2004).
[7] F. Steglich, J. Aarts, C. D. Bredl, W. Lieke, D. Meschede, W. Franz, and H. Schafer, Phys. Rev. Lett. **43**, 1892 (1979).
[8] Y. Kawasaki *et al.*, J. Phys. Soc. Jpn. **73**, 194 (2004).
[9] H. Hegger C. Petrovic, E. G. Moshopoulou, M. F. Hundley, J. L. Sarrao, Z. Fisk, and J. D. Thompson, Phys. Rev. Lett. **84**, 4986 (2000).
[10] T. Muramatsu *et al.*, J. Phys. Soc. Jpn. **70**, 3362 (2001).
[11] B. Bellarbi, A. Benoit, D. Jaccard, J. M. Mignot, and H. F. Braun, Phys. Rev. B **30**, 1182 (1984).
[12] F. Thomas *et al.*, Physica B **186-188**, 303 (1993).
[13] T. Mito, S. Kawasaki, Y. Kawasaki G.-q. Zheng, Y. Kitaoka, D. Aoki, Y. Haga, and Y. Onuki, Phys. Rev. Lett. **90**, 077004 (2003).
[14] S. Kawasaki T. Mito, Y. Kawasaki, G.-q. Zheng, Y. Kitaoka, D. Aoki, Y. Haga, and Y. Onuki, Phys. Rev. Lett. **91**, 137001 (2003).
[15] T. Park *et al.*, Nature (London) **440**, 65 (2006).
[16] G. Knebel, D. Aoki, D. Braithwaite, B. Salce, and J. Flouquet, Phys. Rev. B **74**, 020501 (2006).
[17] T. Moriya and T. Takimoto, J. Phys. Soc. Jpn. **64**, 960 (1995).
[18] S.-C. Zhang, Science **275**, 1089 (1997).
[19] E. Demler, W. Hanke, and S.-C. Zhang, Rev. Mod. Phys. **76**, 909 (2004).
[20] Although the previous work reported that the T_1T-constant behavior is not observed below T_c at $P=2.1$ GPa (Ref. 21), the precise new data at low T have been presented in this work to observe the deviation from the T^3 behavior well below T_c by excluding any heat-up effect in the T_1 measurements in fact.
[21] T. Mito S. Kawasaki, G.-q. Zheng, Y. Kawasaki, K. Ishida, Y. Kitaoka, D. Aoki, Y. Haga, and Y. Onuki, Phys. Rev. B **63**, 220507(R) (2001).
[22] Y. Bang, M. J. Graf, A. V. Balatsky, and J. D. Thompson, Phys. Rev. B **69**, 014505 (2004).
[23] H. Tou *et al.*, J. Phys. Soc. Jpn. **64**, 725 (1995).
[24] The NQR spectrum has four peaks in the incommensurate antiferromagnetic order well above T_c at $P=1.62$ GPa, but only two peaks are observed below T_N at $P=1.82$ GPa, indicating that the commensurate antiferromagnetic structure is realized in the AFM+SC uniformly coexisting phase. Further experiments under pressure are now in progress in order to clarify the detailed P evolution of the magnetic structure.
[25] M. Yashima *et al.*, J. Phys. Soc. Jpn. **73**, 2073 (2004).